Modification of Histones by Sugar *β-N*-Acetylglucosamine (GlcNAc) Occurs on Multiple Residues, Including Histone H3 Serine 10, and Is Cell Cycle-regulated*

Suisheng Zhang‡, Kevin Roche‡1, Heinz-Peter Nasheuer§2, and Noel Francis Lowndes‡3

From the ‡Genome Stability Laboratory and §Cell Cycle Control Laboratory, Center for Chromosome Biology, School of Natural Sciences, National University of Ireland Galway, University Road, Galway, Ireland

The monosaccharide, *β-N*-acetylglucosamine (GlcNAc), can be added to the hydroxyl group of either serines or threonines to generate an *O*-linked *β-N*-acetylglucosamine (*O*-GlcNAc) residue (Love, D. C., and Hanover, J. A. (2005) *Sci. STKE 2005* 312, 1–14; Hart, G. W., Housley, M. P., and Slawson, C. (2007) *Nature* 446, 1017–1022). This post-translational protein modification, termed *O*-GlcNAcylation, is reversible, analogous to phosphorylation, and has been implicated in many cellular processes. Here, we present evidence that in human cells all four core histones of the nucleosome are substrates for this glycosylation in the relative abundance H3, H4/H2B, and H2A. Increasing the intracellular level of UDP-GlcNAc, the nucleotide sugar donor substrate for *O*-GlcNAcylation enhanced histone *O*-GlcNAcylation and partially suppressed phosphorylation of histone H3 at serine 10 (H3S10ph). Expression of recombinant H3.3 harboring an S10A mutation abrogated histone H3 *O*-GlcNAcylation relative to its wild-type version, consistent with H3S10 being a site of histone *O*-GlcNAcylation (H3S10glc). Moreover, *O*-GlcNAcylated histones were lost from H3S10ph immunoprecipitates, whereas immunoprecipitation of either H3K4me3 or H3K9me3 (active or inactive histone marks, respectively) resulted in co-immunoprecipitation of *O*-GlcNAcylated histones. We also examined histone *O*-GlcNAcylation during cell cycle progression. Histone *O*-GlcNAcylation is high in G_1 cells, declines throughout the S phase, increases again during late S/early G_2, and persists through late G_2 and mitosis. Thus, *O*-GlcNAcylation is a novel histone post-translational modification regulating chromatin conformation during transcription and cell cycle progression.

O-GlcNAcylation, analogously to protein phosphorylation, occurs as a reversible post-translational modification of proteins involved in cell signaling, stress responses, and during cell growth (reviewed in Refs. 1, 2). This glycosylation involves the addition of a single sugar molecule, *β-N*-acetylglucosamine, to the hydroxyl group of serine or threonine (termed *O*-GlcNAc). This may lead to a reciprocal regulation of protein function

because phosphorylation and *O*-GlcNAcylation may compete with each other for the same amino acid residue. *O*-GlcNAcylation has also been reported to regulate protein "turnover" by altering the activity of the proteasome or substrates targeted for degradation (3).

The level of *O*-GlcNAcylation is controlled within the cell by two evolutionarily conserved enzymes, a transferase (*O*-linked *β-N*-acetylglucosamine transferase or OGT)[4] and a hydrolase (*O*-linked *β-N*-acetylglucosaminidase, alternatively *O*-GlcNAcase or OGA), which add or remove, respectively, *O*-GlcNAc (4). OGT is present in mammals as a single copy gene on the X chromosome, and its deletion in the mouse results in early (day E5 post-fertilization) embryonic lethality (5). In *Caenorhabditis elegans*, OGT plays a role in insulin resistance as its deletion suppressed the induction of dauer formation in a genetic background defective for insulin signaling (6). Under similar conditions, knock-out of OGA promoted dauer formation (7), supporting an involvement of *O*-GlcNAcylation in metabolic regulation in this animal.

OGT in human cells interacts with phosphoinositide at the plasma membrane, where *O*-GlcNAcylation is believed to attenuate insulin signaling by suppressing the phosphorylation of protein kinase Akt (8). Moreover, *O*-GlcNAcylation may control cell growth by altering the stability of the tumor suppressor p53 (9), as well as the NFκB-IκkB signaling pathway (10, 11). In response to various cellular stresses, an increased level of protein *O*-GlcNAcylation was observed (12). *O*-GlcNAcylation may have an effect on the formation of protein complexes, as has been observed for ribosomal proteins and which, in this case, leads to an alternation of translational activities or RNA decay (13).

Modification of proteins by *O*-GlcNAcylation has been implicated in chromosome biology as this glycosylation is enriched in the condensed and repressed regions of *Drosophila* polytene chromosomes (14). Chromosomal proteins modified by *O*-GlcNAc are exemplified by many transcriptional factors, such as Sp1 (15) and c-Myc (16), as well as p53 (9). A further role for this modification in regulating transcription is suggested by the reciprocal relationship between *O*-GlcNAcylation and elongation-dependent phosphorylation at the C-terminal domain (CTD) of RNA polymerase II (17). A direct role in tran-

scriptional repression is suggested by the observation that the N-terminal tetratricopeptide repeat domain of OGT interacts with a transcriptional repressor, mSin3, which exists in a complex with a histone deacetylase involved in gene silencing (18). Even more intriguingly, the C terminus of OGA contains a domain resembling a histone acetyltransferase domain that has been shown to be capable of acetylating nucleosomal histones *in vitro* (19). Clearly, the associations between OGT and histone deacetylase and OGA and histone acetyltransferase activities suggest reciprocal and reversible control of gene expression.

Two recent observations further highlight the potential for *O*-GlcNAcylation in the regulation of transcription. First, the gene encoding OGT in *Drosophila* has been mapped to a polycomb group (PcG) gene locus termed *super sex combs* (sxc), which is involved in the repression of homeotic genes during the development of this organism (20, 21). Second, *O*-GlcNAcylation of MLL5, a histone lysine methyltransferase, has been shown to lead to dimethylation of H3K4 required for retinoic acid-induced transcription during promyelocyte differentiation (22).

However, despite increasing evidence supporting the involvement of *O*-GlcNAcylation in multiple aspects of chromosome biology, the possibility that the histones proteins may also be the targets for *O*-GlcNAcylation remained to be investigated. This might relate to difficulty in mapping sites of *O*-GlcNAcylation via mass spectrometry due to the labile glycosidic bond and/or low stoichiometry of this modification on some proteins (1, 2). Nevertheless, recent data based on *in silico* analysis of histone post-translational modifications predict the occurrence of histone *O*-GlcNAcylation (23). We therefore used both antibodies and a lectin (wheat germ agglutinin (WGA) with specificity for *O*-GlcNAc to examine histones from human cells for *O*-GlcNAcylation. Here, we report that histones are indeed substrates for *O*-GlcNAcylation. Using both one- and two-dimensional electrophoresis, we determined that all four nucleosomal core histones are *O*-GlcNAcylated in the relative order H3, H4 or H2B, and H2A. Furthermore, we provide multiple lines of evidence that serine 10 of histone H3 is indeed a site of *O*-GlcNAcylation (H3S10glc). Our data are compatible with the possibility of either an *O*-GlcNAc or an *O*-phosphate modification at serine 10 of histone H3. Increased global *O*-GlcNAcylation of all three isoforms of histone H3 resulted in a global loss of a modification indicative of active chromatin (H3K9Ac) and a corresponding global increase of a modification indicative of repressed chromatin (H3K9me3). Finally, histone *O*-GlcNAcylation correlated with progression of cells through the cell cycle. Specifically, histone *O*-GlcNAcylation was high in G_1, globally decreased during S phase but re-emerged in late S/early G_2, and persisted during mitosis. These findings suggest that regulation of histones by *O*-GlcNAcylation plays a regulatory role in chromosome metabolism during the cell cycle, with histone H3S10 being a major site of *O*-GlcNAcylation and global histone *O*-GlcNAcylation being specifically depleted during DNA replication.

EXPERIMENTAL PROCEDURES

Antibodies—The mouse monoclonal antibodies CTD110.6 and RL2 specific to *O*-GlcNAc and the rabbit polyclonal antibodies against histone H3K9me3, H3K4me3, H3K9Ac, and H3S28p were obtained from Abcam (Cambridge, UK). The rabbit polyclonal IgG specific to histone H3S10ph was supplied by Upstate Biotechnology, Inc. (Lake Placid, NY). All antibodies were used according to the manufacturers' recommendations.

Cell Culture—Human HeLa and HEK293 epithelial cells were grown in Dulbecco's modified Eagle's medium (Lonza Walkersville, Inc., MD), supplemented with 10% fetal calf serum (Lonza), and cultured at 37 °C in a humidified atmosphere with 5% CO_2. Human CCRF-*CEM*, acute T lymphoblastic leukemia cell line, and K562, erythroleukemia cells (both from ATCC), were grown in RPMI 1640 medium (Lonza) supplemented with 10% FCS (Lonza) at 37 °C in a humidified atmosphere with 5% CO_2. Treatment with glucosamine was performed with actively growing cells by adding it to the cell culture medium at concentrations of 0, 2.5, 5, and up to 15 mM. The cells were harvested after overnight incubation (>16 h), and whole cell lysates or histones proteins were prepared as described below.

Acid Extraction of Histones—Histone preparation was based on an acid extraction using hydrochloric acid (HCl). The extraction was performed at 4 °C with all buffers supplemented with a protease inhibitor mixture (Roche Applied Science), 1 mM phenylmethanesulfonyl fluoride (PMSF), 1 mM DTT, 1 mM NaF, 0.1 mM sodium orthovanadate (Na_3VO_4), and 80 μM *O*-(2-acetamido-2-deoxy-D-glucopyranosylidene) amino *N*-phenyl-carbamate (Sigma), an inhibitor of *O*-GlcNAcase. The cultured cells were harvested and washed once with PBS, followed by a suspension of cell pellets in 50 mM MES, pH 6.0, 1 M sorbitol, 5 mM $MgCl_2$ and then centrifuged at 1000 $\times$ *g* for 5 min. The cell pellets were lysed by suspending them in 50 mM MES, pH 6.0, 75 mM KCl, 0.5 mM $CaCl_2$, and 0.1% Nonidet P-40 with repeated pipetting, followed by centrifugation at 12,000 $\times$ *g* for 5 min. The resulting pellets were washed in high salt buffer containing 10 mM MES, pH 6.0, 430 mM NaCl, and 0.5% Nonidet P-40 to dissociate weakly interacting proteins and centrifuged at 15,000 $\times$ *g* for 5 min. This high salt wash was repeated twice to minimize contamination with non-histone proteins. Histone proteins in the pellets were then extracted by treatment with 0.25 N HCl (in distilled H_2O) and vigorous vortexing for 15 min, followed by centrifugation at 12,000 $\times$ *g* for 5 min to obtain the histone-enriched supernatants. This acid extraction was repeated twice, and both supernatants were combined, followed by centrifugation at 3000 $\times$ *g* for 5 min to clear the histone extracts. Eight volumes of acetone were then added per 1 volume of clarified histone extract and incubated at −20 °C overnight to precipitate proteins. Acetone-precipitated histones were harvested by centrifugation at 5000 $\times$ *g* for 5 min and washed once with 0.1 N HCl (in acetone) and twice with acetone alone. Histone pellets were air-dried and finally dissolved in a minimal volume of sterile distilled water. Histone preparations were aliquoted and stored at −80 °C until required.

Two-dimensional Gel Electrophoresis of Histones—Analysis of histones by two-dimensional gel electrophoresis was performed using the protocol described by Shechter *et al.* (24). The first dimension of histone separation was obtained by TAU electrophoresis in a short (~10 cm) gel, with a final gel volume of 10 ml that contained 3.6 g of urea, 2.5 ml of a 60:0.4% acrylamide/bisacrylamide solution, 500 μl of glacial acetic acid, 370 μl of Triton X-100; 60 μl of TEMED, and 140 μl of 10% ammonium persulfate. Histones to be loaded onto the TAU gel were mixed with a freshly prepared sample buffer generated as follows: 0.36 g of urea, 100 μl of 0.2% pyronin Y, 50 μl of glacial acetic acid, and 500 μl of 25 mg/ml protamine sulfate in a final volume of 1 ml. TAU gel electrophoresis was performed at 200 V for ~90 min in a buffer of 5% glacial acetic acid. After TAU gel electrophoresis, conventional SDS-PAGE was performed in the second dimension to resolve individual histones and certain isoforms. For the second dimension, one lane from the TAU gel after electrophoresis of the histones was excised and incubated in a buffer containing 2% SDS, 60 mM Tris/HCl, pH 6.8, and 5% β-mercaptoethanol with three changes each of 5 min duration. The equilibrated gel slice was then placed on top of a standard 15% SDS-polyacrylamide gel, followed by an overlay of stack gel solution. After polymerization of the stacking gel, electrophoresis was performed as usual for SDS-PAGE.

Western Blotting—After electrophoresis of histones on TAU gels, histones were transferred to PVDF membranes at 30 V overnight (>16 h) in a buffer of 0.7% acetic acid. Prior to transfer, TAU gels were incubated with 0.7% acetic acid for 15 min to equilibrate with the transfer buffer. After electrophoresis of histones by SDS-PAGE, transfer of proteins to nitrocellulose membranes was performed using standard conditions. For detection of *O*-GlcNAc, the membranes were blocked in 3% BSA and then incubated with the mouse antibody RL2 or CTD110.6, both diluted at 1:1000. Alternatively, a lectin probe specific to *O*-GlcNAc, WGA, coupled with horseradish peroxidase (WGA-HRP, from Alpha Diagnostic, TX) was used at a dilution of 1:1000. Membranes for all other immunodetections were blocked in 3% milk powder with a dilution of antibody 1:2000 for the rabbit polyclonal antibody against H3S10ph and H3S28ph, 1:1000 for the rabbit polyclonal antibody against H3K9ac, and 1:10,000 for the rabbit polyclonal antibody against H3K9me3 and H3K4me3.

Cell Cycle Analysis—A double thymidine (5 mM) block (25) was used to synchronize HeLa cells at the transition from G_1 into S phase as described previously (26). Briefly, blocked cells were allowed to resume the cell cycle by removal of the thymidine-containing medium, extensive washing of the cells with PBS, and replacement with fresh pre-warmed culture medium. Collected cells at each time point were divided into two halves, one for flow cytometry (FACS) and the other for an immediate lysis in SDS-PAGE sampling buffer for analysis by Western blotting. Cells for FACS analysis were collected and immediately fixed in 85% ethanol, stored at −20 °C, and then stained with propidium iodide, followed by the measurement of DNA content in a flow cytometer (FACSCalibur).

As an alternative method for synchronizing cells, the elutriation procedure was used to obtain a cell size-based fractionation of CEM, K562, and HEK293 cells into different phases of the cell cycle as described previously (27). This was performed by loading actively growing cells (2×10^7–10^8) into the standard chamber of an elutriator rotor (JE-5.0, Beckman Coulter), followed by collection of cells at 2200 rpm and increasing the flow rate from 32, 36, and 41–47 ml/min, which fractionated the cells into G_1, S, and G_2 plus mitosis-enriched populations. The collected cells were processed for FACS analysis and Western blot analyses as described above.

Histone Immunoprecipitation—Nuclear extracts of HEK293 cells were used for histone immunoprecipitations. All steps were performed at 4 °C with a supplement of protease inhibitor mixture in all the buffers. After washing with PBS, the collected cell pellets were resuspended in a hypotonic buffer composed of 10 mM Tris/HCl, pH 7.5, 10 mM NaCl, 1.5 mM MgCl$_2$, 0.1% Triton X-100, and protease inhibitor mixture. After centrifugation at 3000 $\times$ g for 5 min, the nuclei pellets were suspended in a buffer of 50 mM Tris/HCl, pH 8.0, 150 mM NaCl, 1 mM EDTA, 0.5 mM DTT, 1% Triton X-100, 0.5% sodium deoxycholate, 0.1% SDS and protease inhibitor mixture, followed by sonication for 6 pulses, each of 6 s duration at an output of 40% in a Branson-250 digital sonifier. After centrifugation of the sonicated nuclear extracts at 20,000 $\times$ g for 5 min, supernatants were divided for incubation with antibodies specific to different histone post-translational modifications. Subsequently, protein G-agarose (20-μl bed, GE Healthcare) was added to each mixture followed by a further incubation for 1 h. The protein G-agarose beads were pelleted by brief centrifugation at 15,000 $\times$ g for 1 min, washed three times with a buffer containing 20 mM Tris/HCl, pH 7.5, 500 mM NaCl, 3 mM MgCl$_2$, 0.2 mM EDTA, 10% glycerol, and 0.1% Nonidet P-40. Immunoprecipitates were finally suspended in a sample buffer for SDS-PAGE, heated at 95 °C for 5 min, and analyzed by SDS-PAGE and Western blotting.

In Vivo Expression of Recombinant Histones—A plasmid vector, pOZ FH-C, for expression of FLAG and HA-tagged wild-type human histone H3.3 in mammalian cells was a kind gift from Prof. Tsuyoshi Ikura (Radiation Biology Centre, Kyoto University). Wild-type H3.3 and its mutant S10A or T11V were synthesized by the gene synthesis service from GENEART (Regensburg, Germany) and subcloned into XhoI and NotI sites of plasmid pOZ FH-C. For *in vivo* expression, plasmids were transfected into HEK293 cells via the CaCl$_2$ method. Cells were harvested 48 h after transfection to prepare whole cell lysates. Immunoprecipitation of recombinant H3.3 was performed as described above with the M2 FLAG immunoaffinity agarose (Sigma).

Expression of Recombinant OGT and in Vitro Assays—A pET plasmid encoding full-length human OGT (116 kDa) was kindly supplied by Prof. J. A. Hanover (Laboratory of Cell Biology and Biochemistry, National Institutes of Health, Bethesda). The full-length OGT gene was then subcloned into a donor plasmid pFastBac^{TM} at the BamHI site for its expression from baculovirus (bacmid, Invitrogen), with a His$_6$ tag at its N terminus for affinity purification on Ni^{2+}-agarose. Insect cells (High 5) 48 h after infection with bacmid expressing OGT were harvested and suspended in a hypotonic buffer (I) of 20 mM Tris/HCl, pH 7.5, 10 mM NaCl, 1.5 mM MgCl$_2$, 0.5 mM DTT, 0.1% Triton X-100 and 10% glycerol for disruption of the cells. The lysates
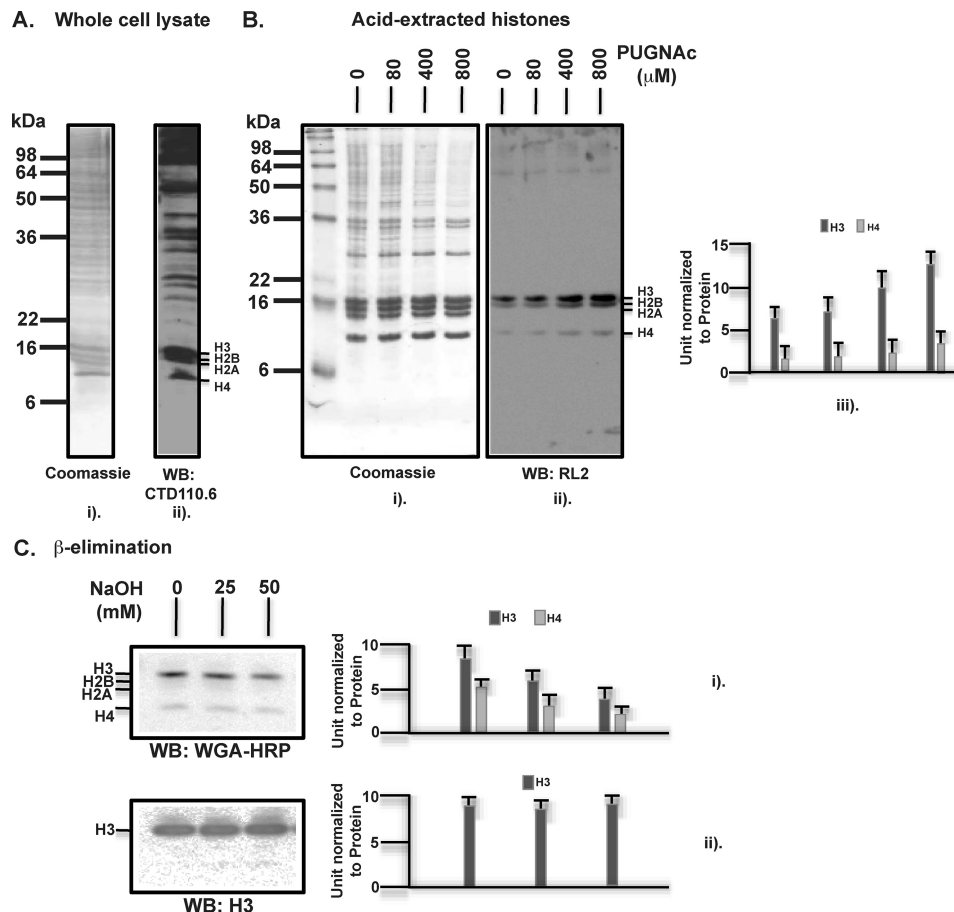
FIGURE 1. **Human histones are post-translationally modified by glycosylation, specifically O-GlcNAcylation.** *A,* whole cell lysates were prepared from cultured HEK293 cells that were immediately denatured in SDS-PAGE sampling buffer at 95 °C for 5 min. After electrophoresis through a 15% SDS-polyacrylamide gel, Western blotting (*WB*) was performed with the mouse monoclonal antibody CTD110.6, specific to *O*-GlcNAc. *B,* histones were prepared by acid extraction from HEK293 cells as described under "Experimental Procedures." *O*-(2-Acetamido-2-deoxy-D-glucopyranosylidene) amino *N*-phenylcarbamate (*PUGNAc*) was included at the indicated concentrations in all the buffers to inhibit *O*-GlcNAcase that removes *O*-GlcNAc. After SDS-PAGE of extracted histones, Western blotting was performed with the mouse monoclonal antibody RL2, also specific to *O*-GlcNAc, which is quantified three times via densitometry and presented in units normalized to the protein levels, the *errors* indicating means ± S.D. *C,* histone *O*-GlcNAcylation was examined for its sensitivity to mild base treatment leading to β-elimination of the *O*-linked GlcNAc. For this purpose, the acid-extracted histones were incubated without or with 25 and 50 mM NaOH for 30 min at 37 °C, followed by SDS-PAGE and Western blotting with a lectin probe WGA-HRP that is also specific to *O*-GlcNAc. A rabbit polyclonal antibody against total histone H3 was used for presenting an input control. Quantifications are presented as above.

were then supplemented with 500 mM NaCl, followed by incubation with rotation at 4 °C for 30 min, and then centrifugation at 15,000 × *g* for 5 min. The obtained supernatants were mixed at 4 °C for 30 min with nickel-agarose pre-equilibrated with a high salt buffer (500 mM NaCl in buffer I). His₆-tagged OGT was eluted with increasing concentrations of imidazole in the same high salt buffer.

Purified OGT (eluted at 80 mM imidazole) was applied to an *in vitro* assay for observing its effect on Aurora B kinase (Abcam), with histone H3 as the substrate. The reaction mixture (10 μl) contained 50 mM Tris/HCl, pH 7.5, 1 mM DTT, 12.5 mM MgCl₂, 100 μM ATP, 100 μM UDP-GlcNAc (donor substrate of OGT, Sigma), recombinant histone H3 (0.1 μg/μl), and different amounts of Aurora B (Abcam) or OGT. When used, [γ-³²P]ATP as a phosphate donor was included at 10 μCi/ per assay (3000 Ci/mmol, PerkinElmer Life Sciences) in addition to the unlabeled ATP given above. After incubation at 37 °C for 30 min, the reaction mixture was mixed with SDS-PAGE loading buffer and then heated at 95 °C for 5 min, followed by electrophoresis and autoradiography, or Western

blotting with a phospho-epitope-specific antibody to examine the phosphorylation.

RESULTS

Human Histones Are O-GlcNAcylated—We initially examined *O*-GlcNAcylation of human histones from whole cell lysates of HEK293 cells. Using an *O*-GlcNAc-specific antibody, CTD110.6, Western blot analysis revealed bands at positions corresponding to core histones (Fig. 1*A*). This putative identification of *O*-GlcNAcylated histone using CTD110.6 was confirmed using RL2 (Fig. 1*B*), an independent monoclonal antibody specific to *O*-GlcNAc. In this experiment, we also enriched the histones using acid extraction, and because the *O*-GlcNAc modification is notoriously labile (1, 2), we used *O*-(2-acetamido-2-deoxy-D-glucopyranosylidene) amino *N*-phenylcarbamate, an inhibitor of the OGA enzyme that removes *O*-GlcNAc. We obtained highly similar data with the RL2 antibody, as well as demonstrating increased histone *O*-GlcNAcylation upon increasing concentration of the OGA inhibitor. These analyses also revealed an apparent order
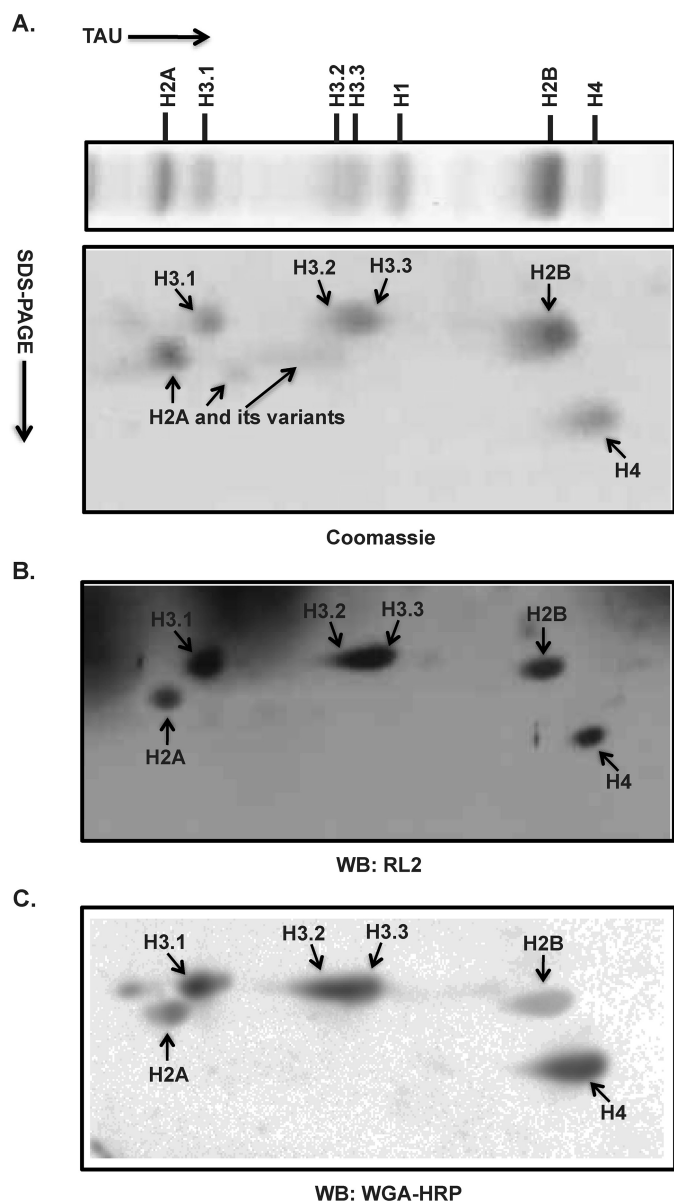
A.

B.

C.

FIGURE 2. **Histone *O*-GlcNAcylation is further resolved using two-dimensional gel electrophoresis.** Acid-extracted histones from HEK293 cells were separated first by TAU gel electrophoresis, followed by a second dimensional separation through 15% SDS-PAGE. Histones after TAU or two-dimensional gel electrophoresis were visualized by Coomassie Blue (*A*) or transferred to a nitrocellulose membrane for Western blot (*WB*) with the antibody RL2 (*B*) or WGA-HRP (*C*), both of which revealed the levels of *O*-GlcNAcylation of individual histones and some of their isoforms or variants, as indicated.

(which was similar with both antibodies) of histone *O*-GlcNAcylation, with histone H3 displaying the most *O*-GlcNAcylation, H4 and H2B being similarly *O*-GlcNAcylated, and H2A *O*-GlcNAcylation only weakly apparent after prolonged exposure (and see below). To further confirm the authenticity of histone *O*-GlcNAcylation, we used a nonimmunological method to detect histone *O*-GlcNAcylation. The lectin WGA is specific to *O*-GlcNAc (1, 2), and when coupled to horseradish peroxidase (WGA-HRP) it can be used in Western analyses to detect *O*-GlcNAcylated protein. WGA-HRP revealed a similar pattern of histone reactivity to the antibodies RL2 or CTD110.6,

although WGA-HRP preferentially detects H4 over H2B (Figs. 1*C* and 2). In addition, in this experiment we also used a mild base treatment (up to 50 mM NaOH) of the acid-extracted histones, as this treatment is known to reduce *O*-linked rather than *N*-linked glycosylation due to the *β*-elimination reaction (28). This mild base treatment significantly diminished the WGA detection of histone *O*-GlcNAcylation by ~50% (see *upper graph* in Fig. 1*C*).

To obtain a higher resolution of individual histones modified by *O*-GlcNAc, and also to further confirm histone *O*-GlcNAcylation, we performed two-dimensional gel electrophoresis with acid-extracted histones (Fig. 2). The first dimension involved a separation based on both the positive charge and hydrophobic properties of histones, termed TAU gel electrophoresis (24). The second dimension separates proteins based on molecular weight using conventional SDS-PAGE. This methodology resolved all histones from the core nucleosome, including H2A and its minor variants, all three H3 variants, H3.1, -3.2, and -3.3, H2B and H4 (Fig. 2*A*). Histones resolved on these two-dimensional gels were transferred to nitrocellulose membrane, followed by detection with either the RL2 (Fig. 2*B*) or CTD110.6 (data not shown) antibodies, which both revealed that the *O*-GlcNAc signal was highest for histone H3 (the sum of all three of its variants), followed by H2B and H4, and finally H2A (Fig. 2*B*). Similar results were also obtained using WGA-HRP to detect *O*-GlcNAcylated histones (Fig. 2*C*), although detection of H2B in these gels with this lectin reagent is relatively weaker than with either of the immunological reagents. Notably, the two-dimensional gel technique greatly facilitates visualization of *O*-GlcNAcylated H2B and H2A that are otherwise difficult to resolve by the one dimensional SDS-PAGE, the latter technique has a lower resolution and more limited loading capacity that together prevent easy detection of weak *O*-GlcNAc signals (see Fig. 1).

Increasing the Cellular Levels of UDP-GlcNAc Results in Enhanced Histone O-GlcNAcylation—Within cells the *O*-GlcNAc donor is the nucleotide-sugar UDP-GlcNAc that is used by OGT to add the GlcNAc moiety to serine or threonine residues in targeted proteins. UDP-GlcNAc is generated in the hexosamine biosynthetic pathway, with its level directly related to that of glucose or glucosamine (1, 2). As a result, increasing the level of glucosamine in cells often increases the stoichiometry of *O*-GlcNAcylation on a modified protein. We therefore treated HEK293 cells with glucosamine at 5 mM during cell culture, followed by acid extraction of histones and examination of histone *O*-GlcNAcylation. Western blot analysis of histones separated by SDS-PAGE revealed a significant enhancement of histone *O*-GlcNAcylation as detected using the RL2 monoclonal antibody (Fig. 3*A*). Quantification of this glucosamine-dependent increase in histone *O*-GlcNAcylation using two-dimensional gels and the RL2 antibody demonstrated a parallel increase of all four core histones (Fig. 3*B*). The glucosamine-stimulated increase in *O*-GlcNAcylation of the core histones further supports our observations on histone *O*-GlcNAcylation.

Serine 10 of Histone H3 Is a Site of Modification by O-GlcNAc— While treating cells with glucosamine to stimulate histone *O*-GlcNAcylation, we noticed a reciprocal relationship
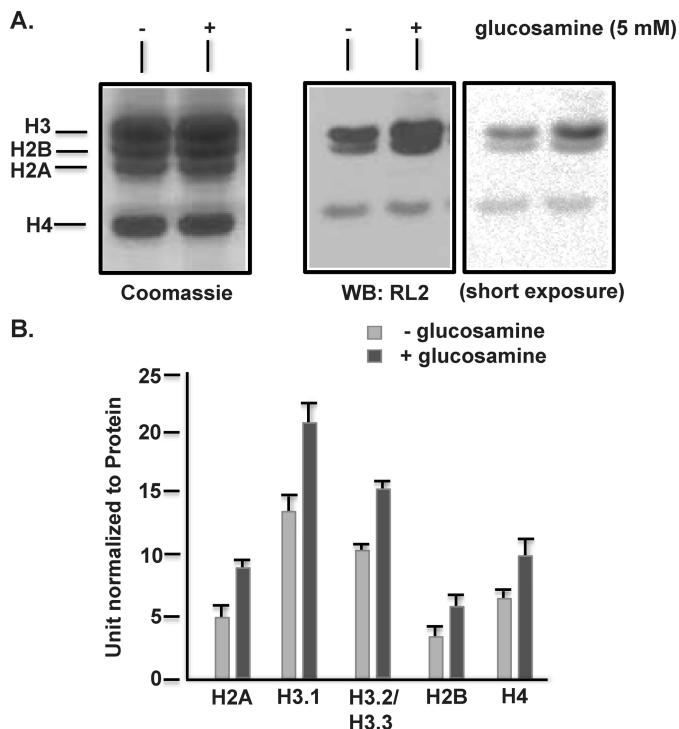
A.

B.

FIGURE 3. **An *in vivo* treatment with glucosamine-enhanced global levels of histone *O*-GlcNAcylation.** *A*, HEK293 cells in culture were treated by glucosamine at 5 mM for 16 h, followed by acid-extraction of histones, SDS-PAGE, and Western blot (*WB*) with antibody RL2 to examine histone *O*-GlcNAcylation. *B*, acid-extracted histones as shown in *A* were separated in parallel by two-dimensional gel electrophoresis as shown in Fig. 2, followed by Western blot with WGA-HRP for detection of individual histone *O*-GlcNAcylation. Quantifications based on densitometry were presented for a comparison of individual histone *O*-GlcNAcylation without or with the glucosamine treatment. Quantifications, in units normalized to the protein levels, are the average and the standard deviation of three experiments.

between histone *O*-GlcNAcylation and phosphorylation of histone H3 on serine 10 (Fig. 4*A*). Increased *O*-GlcNAcylation of all forms of histone H3 detected on one-dimensional TAU gels using antibody RL2 correlated with decreased phosphorylation of H3 forms on serine 10 (H3S10ph). Intriguingly, phosphorylation of serine 28, which is found in a similar sequence context (ARKS) to serine 10, increased upon glucosamine treatment. The relative loss of H3S10ph but increase in H3S28ph upon stimulation of global histone *O*-GlcNAcylation points to a surprisingly distinct regulation of these related post-translational modifications upon glucosamine treatment. We also examined modification of lysine 9 of histone H3, as it is the neighboring residue to serine 10. Interestingly, increased histone H3 *O*-GlcNAcylation upon glucosamine treatment also correlated with a decreased level of H3K9Ac but an increased level of H3K9me3, which correspond to post-translational modification characteristic of active and repressed chromatin respectively (Fig. 4*A*).

The increased histone *O*-GlcNAcylation induced upon treatment with glucosamine observed with acid-extracted histones (Fig. 4*A*) was also confirmed in whole cell extracts and with different concentrations of glucosamine (Fig. 4*B, panel i*). Once more, increasing histone *O*-GlcNAcylation correlated with diminishing levels of phosphorylation of histone H3 serine 10 (Fig. 4*B, panel ii*). Thus, the correlation between increasing

histone *O*-GlcNAcylation and decreasing H3S10ph upon glucosamine treatment is dose-dependent and cannot be an artifact of the acid extraction protocol. Moreover, increasing histone *O*-GlcNAcylation also correlated with decreasing levels of H3K4me3 that is a mark of active chromatin (Fig. 4*B, panel iii*) and increasing levels of H3K9me3, a repressive mark as seen above with the acid-extracted histones (Fig. 4*B, panel iv*).

The identification of specific sites of *O*-GlcNAcylation by mass spectrometry remains challenging due at least in part to the lability of the glycosidic bond once cells are lysed but also the observation that this modification is often present in cells at substoichiometric levels (1, 2). Therefore, as an alternative approach to obtaining evidence directly supporting the modification of histone H3 on serine 10 by *O*-GlcNAcylation, we expressed N-terminally FLAG- and HA-tagged histone H3.3 and its mutant forms S10A and T11V in HEK293 cells. To examine *O*-GlcNAcylation of recombinant H3.3 proteins, immunoprecipitation with an antibody against FLAG tag was performed with sonicated nuclear extracts (Fig. 4*C, panel i*). This led to an enrichment of FLAG-tagged H3.3 proteins in the immunoprecipitates (Fig. 4*C, panel ii*). Probing these anti-FLAG immunoprecipitates with WGA-HRP detected signal with the wild-type H3.3 or the T11V mutant but less from its S10A mutant (Fig. 4*C, panel ii, lower panel*). Together with the reciprocal relationship between global histone *O*-GlcNAcylation and H3S10ph, these genetic data support serine 10 of histone H3 as a site of *O*-GlcNAcylation and suggest an explanation for this reciprocal relationship, *i.e.* serine 10 of histone H3 can either be phosphorylated or glycosylated but not both. Furthermore, the loss of signal in the histone H3.3-S10A mutant relative to the WT indicates that serine 10 is a major site of histone H3.3 *O*-GlcNAcylation, whereas the residual signal in the H3.3-S10A mutant indicates that there are other sites of *O*-GlcNAcylation in this histone on histone H3.3.

Association of Histone O-GlcNAcylation with Active and Inactive Histone Modifications—As a preliminary attempt to examine the possible biological role of histone *O*-GlcNAcylation in the epigenetic regulation of chromosomes, we performed immunoprecipitations using HEK293 nuclear extracts and antibodies against specific histone post-translational modifications (H3S10ph, H3K9me3, and H3K4me3). Consistent with histone H3 serine 10 being a major site of histone H3 *O*-GlcNAcylation, H3S10ph-specific immunoprecipitates lacked appreciable signal when probed with either the anti-GlcNAc antibody, RL2, or the GlcNAc-specific lectin, WGA (Fig. 5*A, panel i*). *O*-GlcNAcylation of H4 was also abrogated in these H3S10ph-specific immunoprecipitates, suggesting that the chromatin fragments precipitated may also have diminished H4 *O*-GlcNAcylation. However, immunoprecipitates of both H3K9me3, a modification associated with inactive or repressed chromatin (see "Discussion"), and H3K4me3, associated with transcriptionally active chromatin (see "Discussion"), both contained *O*-GlcNAcylated histones as assessed by both WGA-HRP and the RL2 monoclonal antibody (Fig. 5*A, panel i*).

To more carefully discern an association of *O*-GlcNAcylation with either of these histone marks, we repeated the immunoprecipitation of H3K4me3 and H3K9me3
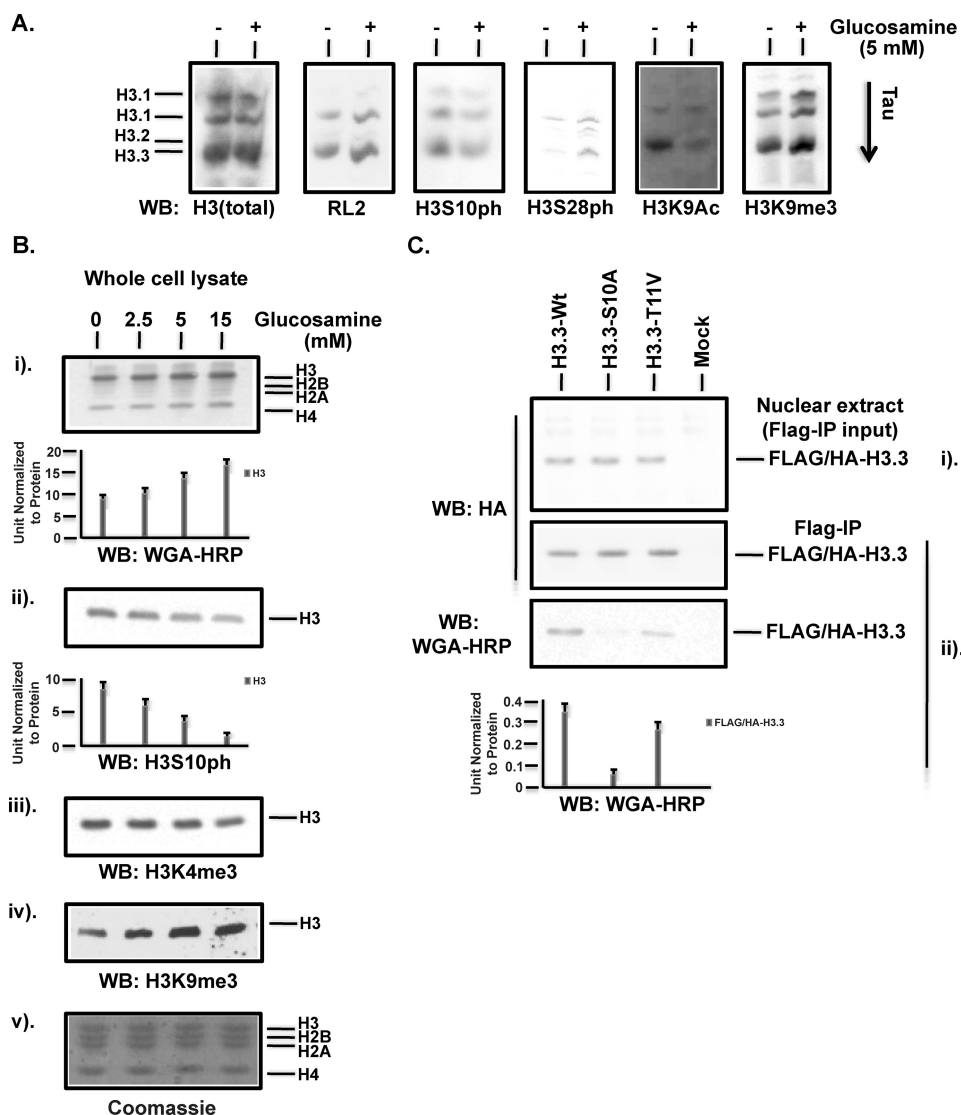
FIGURE 4. **Histone H3 serine 10 is a site of O-GlcNAcylation.** *A,* enhancement of histone *O*-GlcNAcylation by glucosamine is associated with a decreased level of phosphorylation of H3S10 (H3S10ph). Acid-extracted histones from HEK293 cells untreated (−) or treated (+) with glucosamine were separated by TAU gel electrophoresis, followed by Western blotting (*WB*) with antibody RL2 to detect histone *O*-GlcNAcylation and antibodies against various histone H3 post-translational modifications, as indicated, as well as an antibody against total H3. *B,* Western blot of whole cell lysates after glucosamine treatment at the indicated concentrations. Quantifications based on densitometry are presented in units normalized to the protein levels and are the average and the standard deviations of three experiments. SDS-PAGE followed by Coomassie staining indicates total histones. *C,* FLAG- and HA-tagged wild-type H3.3, its S10A and T11V mutant expressed from plasmid pOZ-FH-C transfected into HEK293 cells. Cells at 48 h after transfection were collected for preparing the nuclear extracts (*panel i*) and then immunoprecipitates (*panel ii*) with a mouse monoclonal antibody (M2) against the FLAG tag. Recombinant H3.3 proteins were examined by Western blot with WGA-HRP for detecting *O*-GlcNAc from recombinant H3.3. The WGA signals were quantified and normalized to the signals of anti-HA tag antibody examining recombinant H3.3 in the FLAG tag pulldown.

with nuclear extracts subjected to increasing extents of sonication to minimize incomplete disruption of polynucleosomes. Despite this treatment, the association between H3K9me3 or H3K4me3 modifications with *O*-GlcNAcylated histone H3 was maintained even after extensive sonication (Fig. 5A, panel ii). Moreover, immunoprecipitation of micrococcal nuclease generated mononucleosomes (Fig. 5B, panel i) with the H3K4me3 or H3K9me3-specific antibodies fully supported the previous findings (Fig. 5B, panel ii). Thus, histone *O*-GlcNAcylation can be coupled with post-translational modifications associated with either active or inactive chromatin.

O-GlcNAcylation of Histones Is Cell Cycle-regulated—As a first step in determining the physiological relevance of histone *O*-GlcNAcylation and given its reciprocal relationship with the cell cycle-regulated phosphorylation of histone H3 on serine 10, we investigated histone *O*-GlcNAcylation during cell cycle progression. HeLa cells were arrested at the G_1/S phase boundary by double thymidine block and then released into the cell cycle (see "Experimental Procedures"). Synchrony of cell cycle progression was confirmed using FACS analysis (Fig. 6A) and also assessed by Western blot analysis using the cell cycle marker cyclin A (Fig. 6B) and the mitotic markers corresponding to phosphorylation of histone H3 on serines 10 and 28, *i.e.* H3S10ph and H3S28ph (Fig. 6E).

After release from a double thymidine block, *O*-GlcNAcylation of histone H3 exhibited an initially decreased level during S phase and subsequently increased as cells progressed into G_2 phase and mitosis (Fig. 6C). Although the signal
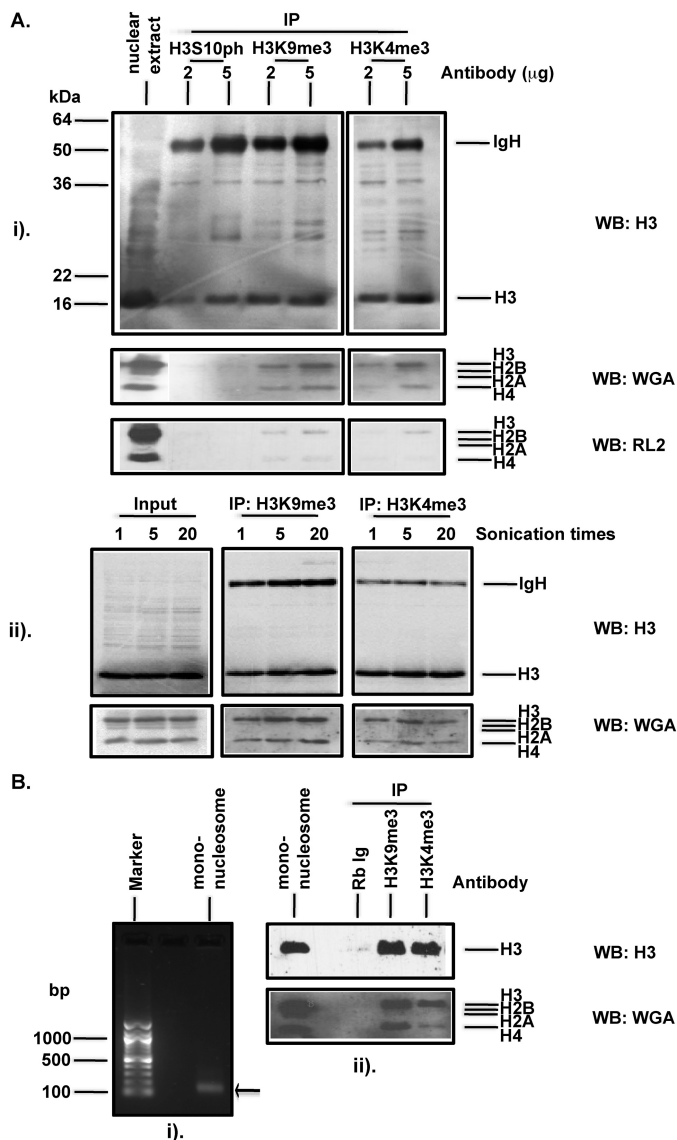
A.

B.

FIGURE 5. **O-GlcNAcylation is associated with both inactive and active marks of histone H3.** *A, panel i,* histone immunoprecipitations (*IP*) using HEK293 nuclear extracts were performed with increasing amounts of antibody against H3S10p, H3K9me3, and H3K4me3 as indicated. Immunoprecipitated histone H3 was examined by Western blot (*WB*) with the antibody against total H3, WGA-HRP, or antibody RL2 to detect histone *O*-GlcNAcylation in the immunoprecipitates. *Panel ii,* histone immunoprecipitations as above and as indicated were performed with nuclear extracts sonicated for indicated number of times, followed by Western blot of immunoprecipitated histone H3 and histone *O*-GlcNAcylation revealed by WGA-HRP. *B,* immunoprecipitation of mononucleosomes derived from micrococcal nuclease digestion of the HEK293 nuclei (*panel i*) and Western blot showing histone *O*-GlcNAcylation associated with mononucleosomes immunoprecipitated with the indicated antibodies (*panel ii*). *Rb Ig* is rabbit immunoglobulin.

corresponding to histone H4 was relatively weaker, we could also discern a regulated pattern of histone H4 *O*-GlcNAcylation. This modification also increased as cells exited S phase; however, unlike H3 *O*-GlcNAcylation, it then decreased concomitantly with the H3S10ph post-translational modification (Fig. 6*E*), which occurs at late stages of mitosis but slightly before the decline in H3S28ph observed in this experiment (Fig. 6*E*). Total histones were analyzed by Coomassie staining (Fig. 6*D*). The repressive and heterochromatin-specific

H3K9me3 post-translational modification, which remained at a constant level after release from the double thymidine block, also serves as a loading control for Western analysis (Fig. 6*E*).

Alternatively, we confirmed the cell cycle regulation of histone *O*-GlcNAcylation by using counter-flow centrifugal elutriation, a physical method that does not require any arresting agents but rather fractionates cells based on their increasing size as they progress through the cell cycle (29).

Fig. 7 shows our results with CCRF-*CEM* (ATCC) cells, a human acute T lymphoblastic leukemia cell line, although similar results were also obtained with HEK293 cells and the K562 (ATCC) erythroleukemia cell line (data not shown). FACS analysis indicates successful fractionation of the asynchronously growing CCRF-CEM cells into seven fractions corresponding to different stages of the cell cycle (Fig. 7*A*). Fraction 1 corresponds to G_1 cells, fractions 2–5 to S phase cells, fraction 6 to mainly G_2 plus mitotic cells with some late S phase cells, and fraction 7 to primarily G_2 plus mitotic cells. S phase is particularly well fractionated in this experiment into early (fractions 2 and 3), middle (fraction 4), and late (fraction 5) stages. The synchrony of the experiment indicated by the FACS data is well supported by Western blot analysis of cyclins (Fig. 7*B*).

Histones were prepared from the elutriated fractions by acid extraction and analyzed by Western blotting (Fig. 7*B*). The histone H3S10ph modification was enriched in those fractions with appreciable amounts of G_2 and mitotic cells, particularly fraction 5–7, whereas total histone H3 was similarly present in all the fractions.

We used WGA-HRP to assess the extent of histone *O*-GlcNAcylation in the elutriated fractions. Although histone H3 is, as usual, more *O*-GlcNAcylated than histone H4, both of these histones have a similar pattern of cell cycle regulation using elutriation. Both appear most *O*-GlcNAcylated in G_1, less *O*-GlcNAcylated throughout S phase, with this modification returning to high levels in fractions 6 and 7, which have the highest proportion of G_2 plus mitotic cells.

To determine whether there are other detectable differences in histone *O*-GlcNAcylation between G_1 and $G_2 + M$ cells, we use the two-dimensional gel technique to examine histone *O*-GlcNAcylation in different elutriated fractions (Fig. 7*C*). The global pattern of histone *O*-GlcNAcylation in these fractions was very similar. All three histone H3 isotypes, H3.1, H3.2 and H3.3, and H2A and H2B are similarly modified in the G_1 (Fig. 7*C, fraction 1*), S (data not shown), and $G_2 + M$ (Fig. 7*C, fraction 7*) cell populations. It is important to point out that examination of global histone *O*-GlcNAcylation during the cell cycle progression cannot rule out any cell cycle-specific modification of a specific histone residue. Therefore, it is possible that at the level of individual residues, there may be other examples of cell cycle regulation that have been missed in our analyses.

In Vitro Reconstitution of Histone H3 O-GlcNAcylation Suppresses Phosphorylation of Histone H3 at Serine 10—In vitro systems using recombinant proteins should prove useful in studies of histone *O*-GlcNAcylation. Furthermore, such a system could provide *in vitro* evidence further supporting a reciprocal relationship between phosphorylation and *O*-GlcNAcylation of histone H3 at serine 10. Therefore, we established OGT-specific and Aurora B-specific *in vitro* his-
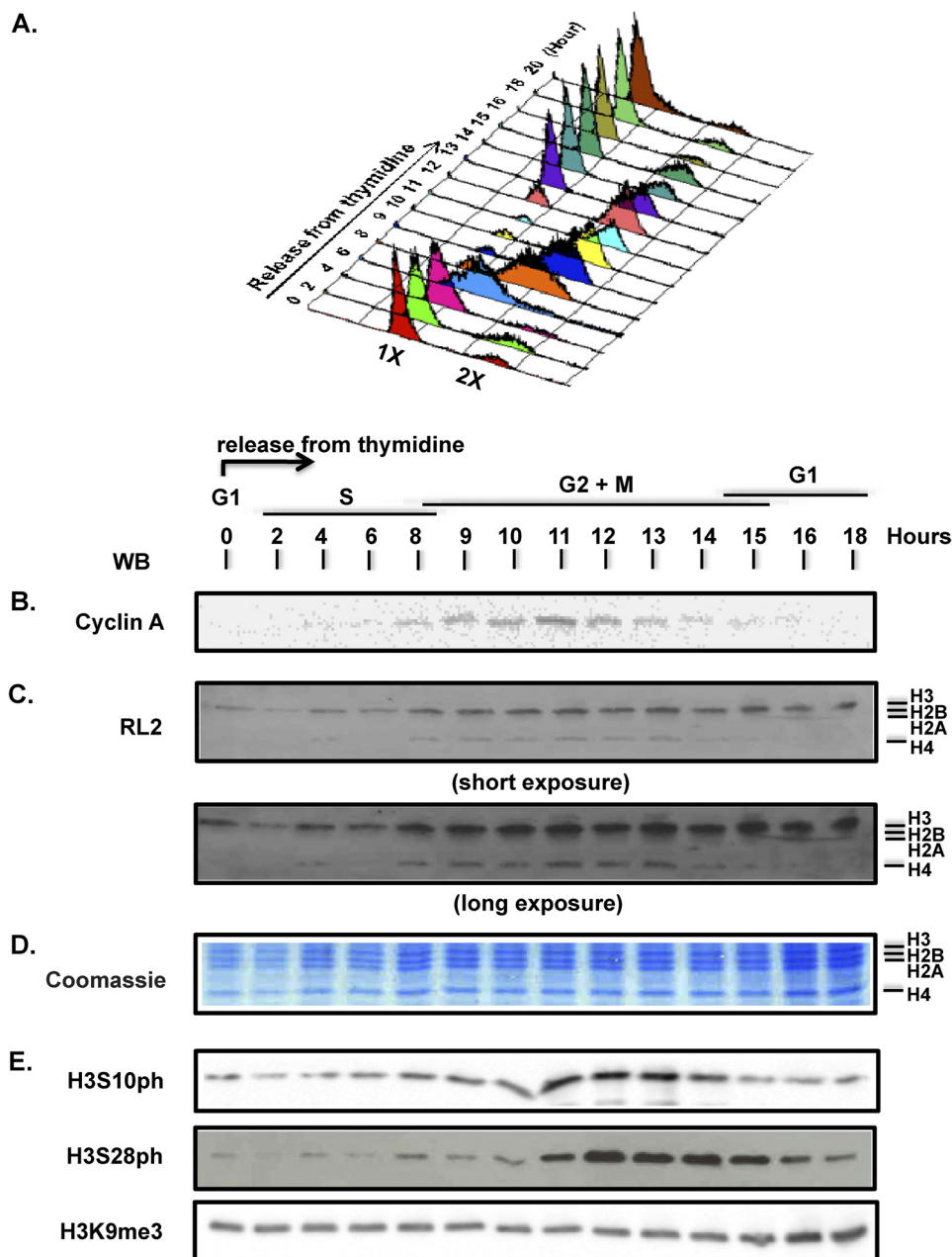
FIGURE 6. **Histone *O*-GlcNAcylation is cell cycle-regulated as assessed by double thymidine block and release.** HeLa cells were synchronized by a double treatment with thymidine to block cell cycle at the transition of G_1 to S phase. Cell cycle was followed at the indicated time points after release from the thymidine block. *A*, FACS profiles showing a progression through the cell cycle. *B*, Western blot (*WB*) using whole cell lysates and an antibody against cyclin A. Cell cycle phases estimated from the FACS data, cyclin A, and H3S10ph (see below) are indicated *above* the cyclin A blot. *C*, histone *O*-GlcNAcylation examined with the antibody RL2. *D*, histones visualized by Coomassie-staining and SDS-PAGE. *E*, Western blot showing the histone H3 post-translational modifications H3S10ph, H3S28ph, and H3K9me3. Coomassie-stained total histones and H3K9me3 serve as loading controls.

tone H3 *O*-GlcNAcylation and kinase assays. Aurora B is known to phosphorylate serine 10 of histone H3 and associates with OGT in a physical complex that might contribute to the regulation of the cell cycle progression (see "Discussion"). Therefore, we expressed recombinant N-terminal His_6-tagged OGT from baculovirus in insect cells and purified the protein on nickel-agarose (Fig. 8*A*). For the Aurora B-specific kinase assay, we used radiolabeled ATP as the phosphate donor and recombinant histone H3 as the phosphate receiver, and we detected histone phosphorylation by both autoradiography (Fig. 8*B*, *panel i*) and Western blotting (Fig. 8*B*, *panel ii*). Addi-

tion of OGT to the Aurora B-specific kinase reaction suppressed both total and serine 10-specific phosphorylation of histone H3 (Fig. 8*B*, *panels i* and *ii*). Thus, OGT can suppress Aurora B-dependent *in vitro* phosphorylation of recombinant histone H3 at serine 10. This inhibition depended upon active OGT because, after heat inactivation, the enzyme did not affect the phosphorylation of H3 by Aurora B (Fig. 8*B*, *panel iii*). Furthermore, increasing OGT-specific *in vitro* *O*-GlcNAcylation of recombinant histone H3 with increasing input of recombinant OGT was observed by Western blotting (Fig. 8*B*, *panel ii*, *upper panel*). These *in vitro* results are consistent with the
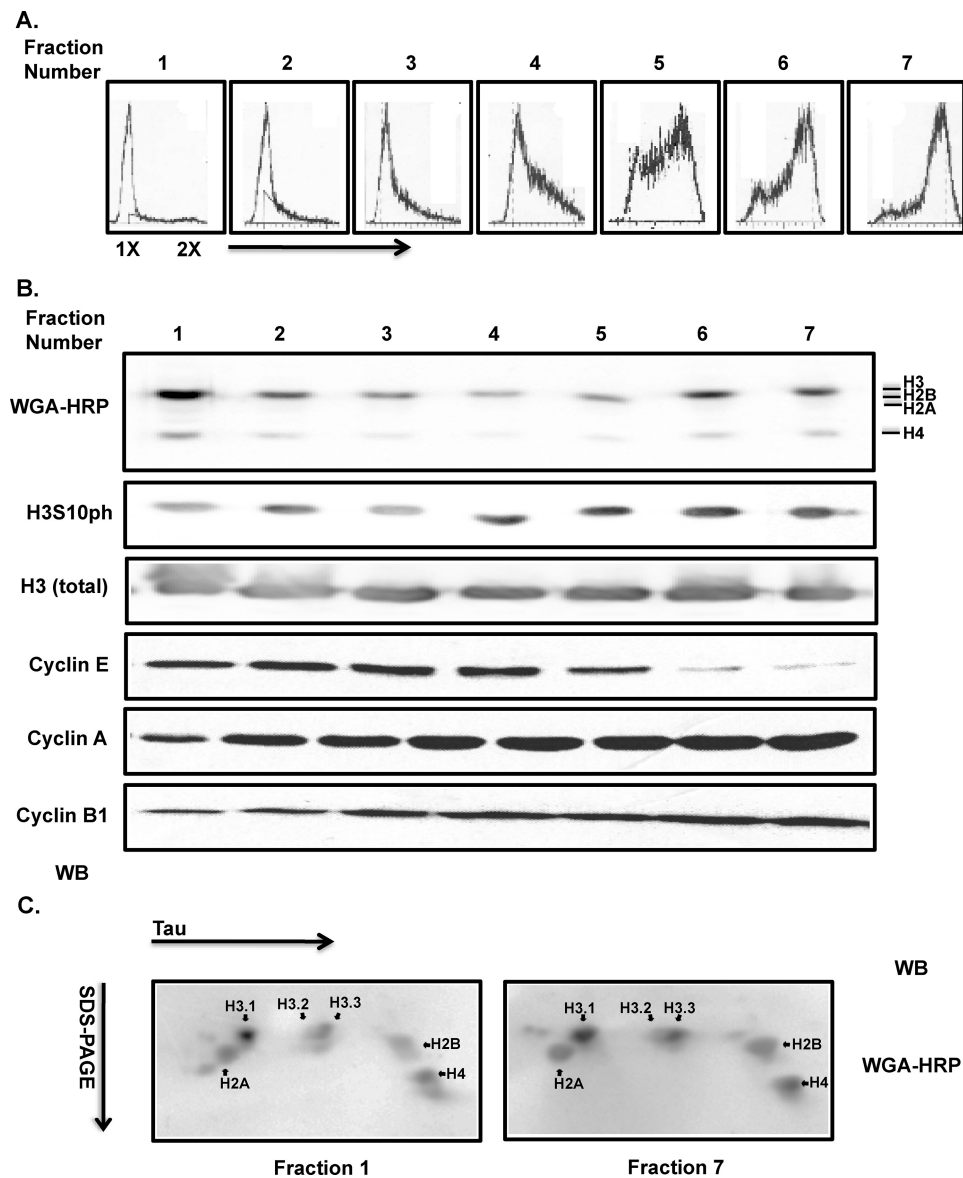
FIGURE 7. **Histone *O*-GlcNAcylation is cell cycle-regulated as assessed by centrifugal elutriation.** Asynchronously growing human acute T lymphoblastic leukemia cells, CCRF-CEM, were loaded into an elutriator rotor, and the flow rate was increased in steps to elute small to large cells. *A*, FACS analysis of the seven eluted fractions indicates successful cell cycle fractionation. *B*, Western blot (*WB*) analyses of the indicated proteins after SDS-PAGE. Histones were prepared by acid extraction and detected using WGA-HRP and antibodies against H3S10ph, total H3, cyclin E, cyclin A, and cyclin B1 as indicated. *C*, *O*-GlcNAcylation of histones prepared from G_1 (*fraction 1*) and G_2 + M (*fraction 7*) cells assessed by two-dimensional gel electrophoresis and Western blotting with WBA-HRP. Note that the faint spot below and to the left of the H2A spot that is visible in fraction 1 is normally not visible in these two-dimensional gels (24) and is either a gel artifact or possibly a minor histone variant specific to G_1.

existence *in vivo* of a reciprocal relationship between these two enzymes targeting serine 10 of histone H3 for distinct modifications.

DISCUSSION

This work presents primary evidence that serine and threonine residues in histone proteins are modified by the post-translational addition of an *O*-linked monosaccharide, β-*N*-acetylglucosamine (termed *O*-GlcNAc). First, we find that glycosylation by *O*-GlcNAcylation occurs on all four-core histones to varying extents in the relative order H3, H2B, or H4 and H2A. Second, increased global *O*-GlcNAcylation of all three isoforms of histone H3 results in global loss of a modification indicative of active chromatin (H3K9Ac) and a corre-

sponding global increase of a modification indicative of repressed chromatin (H3K9me3). Third, serine 10 of histone H3 is a specific and major site of histone H3 *O*-GlcNAcylation that is in competition with phosphorylation of this residue. This reciprocal relationship between *O*-GlcNAcylation and phosphorylation at serine 10 (Ser-10) of histone H3 may exemplify a "Yin-Yang" model involving these two post-translational modifications competing with each other for the same amino acid to modulate protein function (30). Finally, histone *O*-GlcNAcylation is cell cycle-regulated, being globally decreased in abundance during S phase but increasing from late S/early G_2 into mitosis and persisting into the subsequent G_1 phase.

Our observations that histone *O*-GlcNAcylation varied in level during cell cycle progression and overlapped with phos-
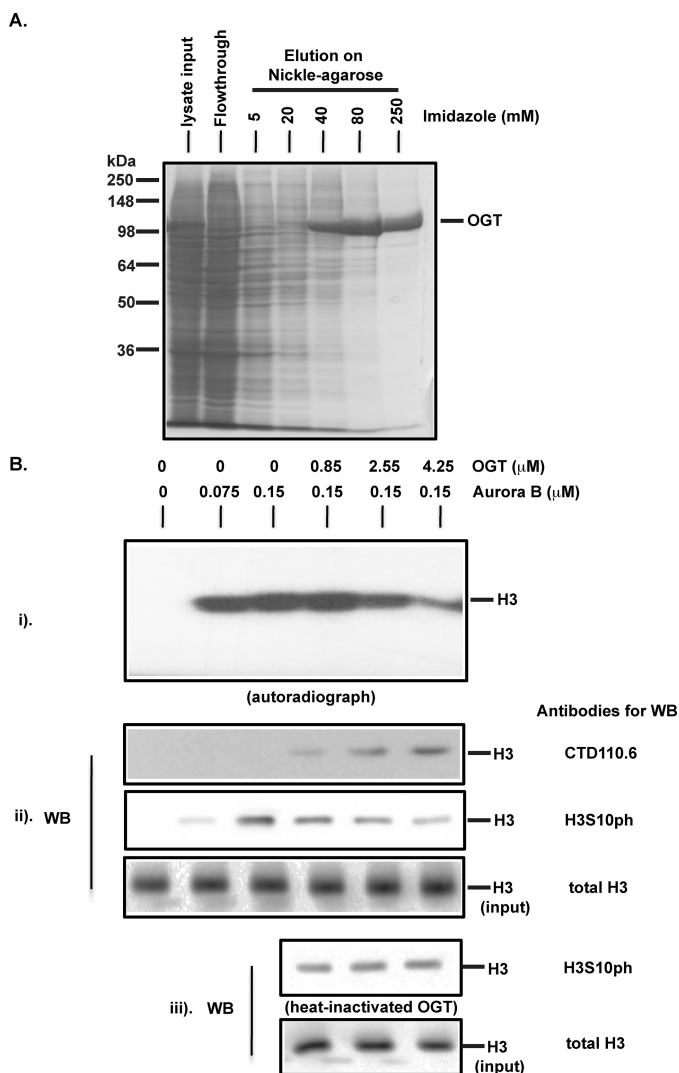
A.

B.

FIGURE 8. **OGT suppressed phosphorylation of histone H3 at serine 10 by Aurora B *in vitro*.** *A,* purification of baculovirus-expressed OGT on Ni^{2+}-agarose. Proteins from whole lysate, flow-through, and fractions eluted at the indicated concentrations of imidazole were examined by SDS-PAGE followed by Coomassie stain. *B,* effect of OGT on phosphorylation of histone H3 by Aurora B. For all the reactions, UDP-GlcNAc was included in the assay mixtures as described under "Experimental Procedures" (*panel i*). Aurora B kinase assay performed with [γ-^{32}P]ATP as the phosphate donor. *Panel ii,* Aurora B kinase assay performed with unlabeled ATP (cold) and phosphorylation examined by Western blotting (*WB*) with antibody specifically recognizing phosphorylated serine 10 of H3. The *O*-GlcNAcylation of histone H3 by OGT was examined with the anti-O-GlcNAc antibody CTD110.6. Histone H3 as substrate in the assays was presented by Western blot with an antibody against unmodified H3. *Panel iii,* as a control of OGT activity, the protein was heated at 95 °C for 5 min before addition to the assay mixtures.

phorylation of histone H3 on Ser-10 or Ser-28 is suggestive of physiological significance for this modification. Phosphorylation of H3 at Ser-10 and Ser-28, as well as two threonine residues, Thr-3 and Thr-11, has been reported to be regulated during late G$_2$ and mitosis, although the precise function of these histone phosphorylations remains mysterious (31). Two possibilities have been suggested. First, phosphorylation of the N-terminal tail of histone H3 may be required for condensation and segregation of mitotic chromosomes. A second proposal is that these modifications serve as a mark indicating that chromosomes are ready for separation, the so-called "ready produc-

tion" hypothesis (32). Adding further complexity, phosphorylation of H3 may work in combination with other histone modifications that ultimately result in the correct mitotic chromosome configuration required for the passage through the spindle assembly checkpoint (33).

The findings reported here indicate that replication of chromosomal DNA is accompanied by a global change of histone modification, specifically decreased *O*-GlcNAcylation. We hypothesize that removal of histone *O*-GlcNAcylation during S phase may lead to greater access of chromatin for the DNA replication machinery.

Modification of histone H3 serine 10 by phosphorylation has also been shown to negatively regulate modification of, or disrupt binding of effector proteins to, neighboring residues. For example, methylation of the adjacent lysine 9 residue by the H3K9 methyltransferase, Suv3-9 (34), is inhibited by phosphorylation of serine 10, probably due to limited accessibility of Lys-9 once serine 10 is phosphorylated (35). Phosphorylation of H3S10 also leads to dissociation of heterochromatin-binding protein 1 (HP1) that is otherwise bound to methylated lysine 9 (36). Moreover, recent evidence has established that certain RNA splicing factors (SRp20 and ASF/SF2) that associate with interphase chromosomes, where they are proposed to have "chromatin sensor" activity, are also lost from chromosomes upon phosphorylation of histone H3 on serine 10 (37). With respect to mitosis, H3S10 phosphorylation may, by a currently unknown mechanism, disrupt normal interphase chromatin structure, perhaps by causing the dissociation of factors such as SRp20 and ASF/SF2. H3S10ph-mediated dissociation of such factors might then promote recruitment of the chromosome condensing machinery for the compaction of mitotic chromosomes (38). We propose that antagonism of histone H3 phosphorylation at serine 10 by *O*-GlcNAcylation of the same residue may promote balanced condensation and/or segregation of chromosomes during mitosis, by locally and dynamically regulating the chromatin fiber.

A role for *O*-GlcNAcylation of non-histone proteins in the regulation of mitosis is indicated by the observation that OGT localizes to the midbody during telophase as part of a multicomponent complex. In addition to OGT, this complex also included OGA, Aurora B kinase, and protein phosphatase 1 (39). It is likely that this complex may coordinate dynamic *O*-GlcNAc and *O*-phosphate cycling at the mid-body to regulate cytokinesis and the exit from mitosis. *O*-GlcNAcylation of histone H3 at serine 10 may occur in a similar enzymatic context in which there is a reciprocal interplay between OGT/OGA and Aurora B kinase/PP1, the major kinase and phosphatase responsible for the mitotic phosphorylation and post-mitotic de-phosphorylation of H3S10.

Although H3S10 phosphorylation is associated with mitotic chromosomes that are in a highly condensed state, the same histone modification is also involved in transcription related to de-condensed chromosomes during interphase (40, 41). Emerging evidence favors a role for OGT in transcriptional repression (18, 20, 21); therefore, it is reasonable to suggest that *O*-GlcNAcylation of H3S10 is involved in the formation of inactive or repressed chromatin by counteracting phosphorylation of the same residue (42). Phosphorylation of H3S10 has been

shown to recruit the transcriptional activator and histone acetyltransferase, Gcn5, leading to acetylation of H3K9 and H3K14 (43, 44). Phosphorylated H3S10 has also been shown to recruit a phosphospecific binding protein, 14-3-3, which may in turn promote release of HP1 proteins or, alternatively, provide a platform for additional transcriptional factors, as has recently been shown for the H4K16 histone acetyltransferase, hMOF (45–47).

Moreover, rapidly inducible transcriptional responses, such as those at heat-shock loci, require H3S10 phosphorylation to target a serine 2-specific CTD kinase, termed P-TEFb (positive transcription elongation factor b), which in turn promotes the release of the paused RNA polymerase II into the elongation phase of RNA synthesis (48, 49). We speculate that *O*-GlcNAcylation of histones at residues including H3S10 may function to counteract the varied effects of H3S10ph on transcription. With respect to genes such as those regulated by heat shock where regulation of RNA polymerase II occurs at the initiation-to-elongation transition, *O*-GlcNAcylation of H3S10 might also be related to earlier reports that *O*-GlcNAcylation of RNA polymerase II at serine residues of its CTD heptapeptide tandem repeats (17) inhibits phosphorylation of these repeats and thereby inhibits RNA polymerase II transcriptional cycling (50, 51).

We found that histone *O*-GlcNAcylation was associated with both H3K9me3 and H3K4me3, marks delimiting repressed and active chromatin, respectively (52). Thus, histone *O*-GlcNAcylation should not be considered as exclusively a repressive mark, and indeed a recent study in *C. elegans* indicates that *O*-GlcNAcylation of proteins cycles dynamically at many promoters (53). One possibility is that the association of histone *O*-GlcNAcylation with histone modifications characteristic of both repressed and active chromatin may be indicative of functions in rapid switching between the inactive and active state of chromatin. In this respect, transcriptionally poised RNA polymerase II is already known to be associated with both an active mark (H3K4me3) and a repressive mark (H3K27me3) at certain promoters, the so-called "bivalent" modification (54, 55). If at some promoters GlcNAcylation of H3S10 can work synergistically with the repressive mark, H3K27me3, this might explain our observation that glucosamine-induced histone *O*-GlcNAcylation led to decreased phosphorylation at H3S10 but increased phosphorylation at H3S28. H3S28ph could antagonize the repressive H3K27me3 modification to compensate for increased H3S10glc-dependent repression.

The regulation of transcription through post-translational modification of serine 10 of histone H3 is no doubt highly complex and involved in many signaling pathways that respond to multiple intra- or extracellular stimuli (56, 57). For example, H3S10 phosphorylation has been implicated in expression of NFκB-responsive genes (58), stress responses (59), insulin signaling (60), development (61), and oncogenic transformation (62). Coincidentally, many of these processes are also regulated by *O*-GlcNAcylation (see Introduction) (1–3). The future development of reagents capable of selectively recognizing specific sites of *O*-GlcNAcylation will be required to determine the precise functions of specific sites of histone *O*-GlcNAcylation.

During submission of this study, the Hart group reported *O*-GlcNAcylation of histones, with a specific focus on three sites of *O*-GlcNAcylation on histones H2A (T101glc), H2B (S36glc), and H4 (S47glc) (63). Our work is focused on *O*-GlcNAcylation of histone H3 and is complementary to the earlier report. Together these studies strongly support the identification of *O*-GlcNAcylation as a novel post-translational modification of histone proteins, further expanding the repertoire of histone modifications.

REFERENCES

1. Love, D. C., and Hanover, J. A. (2005) *Sci. STKE 2005,* re13
2. Hart, G. W., Housley, M. P., and Slawson, C. (2007) *Nature* **446,** 1017–1022
3. Zachara, N. E., and Hart, G. W. (2004) *Trends Cell Biol.* **14,** 218–221
4. Hurtado-Guerrero, R., Dorfmueller, H. C., and van Aalten, D. M. (2008) *Curr. Opin. Struct. Biol.* **18,** 551–557
5. Shafi, R., Iyer, S. P., Ellies, L. G., O'Donnell, N., Marek, K. W., Chui, D., Hart, G. W., and Marth, J. D. (2000) *Proc. Natl. Acad. Sci. U.S.A.* **97,** 5735–5759
6. Hanover, J. A., Forsythe, M. E., Hennessey, P. T., Brodigan, T. M., Love, D. C., Ashwell, G., and Krause, M. (2005) *Proc. Natl. Acad. Sci. U.S.A.* **102,** 11266–11271
7. Forsythe, M. E., Love, D. C., Lazarus, B. D., Kim, E. J., Prinz, W. A., Ashwell, G., Krause, M. W., and Hanover, J. A. (2006) *Proc. Natl. Acad. Sci. U.S.A.* **103,** 11952–11957
8. Yang, X., Ongusaha, P. P., Miles, P. D., Havstad, J. C., Zhang, F., So, W. V., Kudlow, J. E., Michell, R. H., Olefsky, J. M., Field, S. J., and Evans, R. M. (2008) *Nature* **451,** 964–979
9. Yang, W. H., Kim, J. E., Nam, H. W., Ju, J. W., Kim, H. S., Kim, Y. S., and Cho, J. W. (2006) *Nat. Cell Biol.* **8,** 1074–1083
10. Kawauchi, K., Araki, K., Tobiume, K., and Tanaka, N. (2009) *Proc. Natl. Acad. Sci. U. S. A.* **106,** 3431–3436
11. Yang, W. H., Park, S. Y., Nam, H. W., Kim, do, H., Kang, J. G., Kang, E. S., Kim, Y. S., Lee, H. C., Kim, K. S., and Cho, J. W. (2008) *Proc. Natl. Acad. Sci. U.S.A.* **105,** 17345–17350
12. Zachara, N. E., O'Donnell, N., Cheung, W. D., Mercer, J. J., Marth, J. D., and Hart, G. W. (2004) *J. Biol. Chem.* **279,** 30133–30142
13. Ohn, T., Kedersha, N., Hickman, T., Tisdale, S., and Anderson, P. (2008) *Nat. Cell Biol.* **10,** 1224–1231
14. Kelly, W. G., and Hart, G. W. (1989) *Cell* **57,** 243–251
15. Yang, X., Su, K., Roos, M. D., Chang, Q., Paterson, A. J., and Kudlow, J. E. (2001) *Proc. Natl. Acad. Sci. U.S.A.* **98,** 6611–6616
16. Chou, T. Y., Dang, C. V., and Hart, G. W. (1995) *Proc. Natl. Acad. Sci. U.S.A.* **92,** 4417–4421
17. Comer, F. I., and Hart, G. W. (2001) *Biochemistry* **40,** 7845–7852
18. Yang, X., Zhang, F., and Kudlow, J. E. (2002) *Cell* **110,** 69–80
19. Toleman, C., Paterson, A. J., Whisenhunt, T. R., and Kudlow, J. E. (2004) *J. Biol. Chem.* **279,** 53665–53673
20. Sinclair, D. A., Syrzycka, M., Macauley, M. S., Rastgardani, T., Komljenovic I., Vocadlo, D. J., Brock, H. W., and Honda, B. M. (2009) *Proc. Natl. Acad. Sci. U.S.A.* **106,** 13427–13432
21. Gambetta, M. C., Oktaba, K., and Müller J. (2009) *Science* **325,** 93–96
22. Fujiki, R., Chikanishi, T., Hashiba, W., Ito, H., Takada, I., Roeder, R. G., Kitagawa, H., and Kato, S. (2009) *Nature* **459,** 455–459
23. Kaleem, A., Hoessli, D. C., Ahmad, I., Walker-Nasir, E., Nasim, A., Shakoori, A. R., and Nasir-ud-Din (2008) *J. Cell. Biochem.* **103,** 835–851
24. Shechter, D., Dormann, H. L., Allis, C. D., and Hake, S. B. (2007) *Nat. Protoc.* **2,** 1445–1457
25. Bootsma, D., Budke, L., and Vos, O. (1964) *Exp. Cell Res.* **33,** 301–309
26. Bauerschmidt, C., Pollok, S., Kremmer, E., Nasheuer, H. P., and Grosse, F. (2007) *Genes Cells* **12,** 745–758

27. Dehde, S., Rohaly, G., Schub, O., Nasheuer, H. P., Bohn, W., Chemnitz, J., Deppert, W., and Dornreiter, I. (2001) *Mol. Cell. Biol.* **21,** 2581–2593

28. Zachara, N. E., Cole, R. N., Hart, G. W., and Gao, Y. (2002) *Curr. Protocols Mol. Biol.* **57,** (suppl.) 17.6.1–17.6.22

29. Pretlow, T. G., 2nd, and Pretlow, T. P. (1979) *Cell Biophys.* **1,** 195–210

30. Wang, Z., Gucek, M., and Hart, G. W. (2008) *Proc. Natl. Acad. Sci. U.S.A.* **105,** 13793–13798

31. Pérez-Cadahía, B., Drobic, B., and Davie, J. R. (2009) *Biochem. Cell Biol.* **87,** 695–709

32. Prigent, C., and Dimitrov, S. (2003) *J. Cell Sci.* **116,** 3677–3685

33. Markaki, Y., Christogianni, A., Politou, A. S., and Georgatos, S. D. (2009) *J. Cell Sci.* **122,** 2809–2819

34. Rea, S., Eisenhaber, F., O'Carroll, D., Strahl, B. D., Sun, Z. W., Schmid, M., Opravil, S., Mechtler, K., Ponting, C. P., Allis, C. D., and Jenuwein, T. (2000) *Nature* **406,** 593–599

35. Duan, Q., Chen, H., Costa, M., and Dai, W. (2008) *J. Biol. Chem.* **283,** 33585–33590

36. Hirota, T., Lipp, J. J., Toh, B. H., and Peters, J. M. (2005) *Nature* **438,** 1176–1180

37. Loomis, R. J., Naoe, Y., Parker, J. B., Savic, V., Bozovsky, M. R., Macfarlan, T., Manley, J. L., and Chakravarti, D. (2009) *Mol. Cell* **33,** 450–461

38. Giet, R., and Glover, D. M. (2001) *J. Cell Biol.* **152,** 669–682

39. Slawson, C., Lakshmanan, T., Knapp, S., and Hart, G. W. (2008) *Mol. Biol. Cell* **19,** 4130–4140

40. Nowak, S. J., and Corces, V. G. (2004) *Trends Genet.* **20,** 214–220

41. Johansen, K. M., and Johansen, J. (2006) *Chromosome Res.* **14,** 393–404

42. Campos, E. I., and Reinberg, D. (2009) *Annu. Rev. Genet.* **43,** 559–599

43. Lo, W. S., Trievel, R. C., Rojas, J. R., Duggan, L., Hsu, J. Y., Allis, C. D., Marmorstein, R., and Berger, S. L. (2000) *Mol. Cell* **5,** 917–926

44. Clements, A., Poux, A. N., Lo, W. S., Pillus, L., Berger, S. L., and Marmorstein, R. (2003) *Mol. Cell* **12,** 461–473

45. Macdonald, N., Welburn, J. P., Noble, M. E., Nguyen, A., Yaffe, M. B., Clynes, D., Moggs, J. G., Orphanides, G., Thomson, S., Edmunds, J. W., Clayton, A. L., Endicott, J. A., and Mahadevan, L. C. (2005) *Mol. Cell* **20,** 199–211

46. Winter, S., Simboeck, E., Fischle, W., Zupkovitz, G., Dohnal, I., Mechtler, K., Ammerer, G., and Seiser, C. (2008) *EMBO J.* **27,** 88–99

47. Zippo, A., Serafini, R., Rocchigiani, M., Pennacchini, S., Krepelova, A., and Oliviero, S. (2009) *Cell* **138,** 1122–1136

48. Ivaldi, M. S., Karam, C. S., and Corces, V. G. (2007) *Genes Dev.* **21,** 2818–2831

49. Nowak, S. J., and Corces, V. G. (2000) *Genes Dev.* **14,** 3003–3013

50. Hartzog, G. A., and Tamkun, J. W. (2007) *Genes Dev.* **21,** 3209–3213

51. Egloff, S., and Murphy, S. (2008) *Trends Genet.* **24,** 280–288

52. Noma, K., Allis, C. D., and Grewal, S. I. (2001) *Science* **293,** 1150–1155

53. Love, D. C., Ghosh, S., Mondoux, M. A., Fukushige, T., Wang, P., Wilson, M. A., Iser, W. B., Wolkow, C. A., Krause, M. W., and Hanover, J. A. (2010) *Proc. Natl. Acad. Sci. U.S.A.* **107,** 7413–7418

54. Hublitz, P., Albert, M., and Peters, A. H. (2009) *Int. J. Dev. Biol.* **53,** 335–354

55. Mellor, J., Dudek, P., and Clynes, D. (2008) *Curr. Opin. Genet. Dev.* **18,** 116–122

56. Bode, A. M., and Dong, Z. (2005) *Sci. STKE 2005,* re4

57. Vermeulen, L., Vanden Berghe, W., Beck, I. M., De Bosscher, K., and Haegeman, G. (2009) *Trends Biochem. Sci.* **34,** 311–318

58. Yamamoto, Y., Verma, U. N., Prajapati, S., Kwak, Y. T., and Gaynor, R. B. (2003) *Nature* **423,** 655–659

59. He, Z., Ma, W. Y., Liu, G., Zhang, Y., Bode, A. M., and Dong, Z. (2003) *J. Biol. Chem.* **278,** 10588–10593

60. Kabra, D. G., Gupta, J., and Tikoo, K. (2009) *Biochim. Biophys. Acta* **1792,** 574–583

61. Teng, H., Ballim, R. D., Mowla, S., and Prince, S. (2009) *J. Biol. Chem.* **284,** 26368–26376

62. Zippo, A., De Robertis, A., Serafini, R., and Oliviero, S. (2007) *Nat. Cell Biol.* **9,** 932–944

63. Sakabe, K., Wang, Z., and Hart, G. W. (2010) *Proc. Natl. Acad. Sci. U.S.A.* **107,** 19915–19920